The PMHT for Passive Radar in a DAB/DVB Network

SORA CHOI
PETER WILLETT
SHENGLI ZHOU

Passive radar using Digital Audio/Video Broadcast (DAB/DVB) signals with Orthogonal Frequency Division Multiplexing (OFDM) must contend with measurements of range and range-rate only (no, or very poor, angular information) and must deal with an added and unwonted measurement-illuminator-target association. But tracking systems using modified Joint Probabilistic Data Association (JPDA) filters and using particle filters have been suggested and seem to work effectively to maintain tracks directly in the Cartesian domain. In this correspondence, we present an alternative Cartesian-domain tracking algorithm a version of the Probabilistic Multi-Hypothesis Tracker (PMHT), to contend with the extra-list data association in a natural way.

Manuscript received December 6, 2013; revised March 7, 2014; released for publication March 7, 2014.

Refereeing of this contribution was handled by Huimin Chen.

This work was supported by the Office of Naval Research under contracts N00014-09-10613, N00014-10-10412 & N000014-13-1-0231.

Authors' address: Department of Electrical and Computer Engineering, University of Connecticut, 371 Fairfield Way, U-4157, Storrs, Connecticut 06269 USA, (E-mail: {soc07002, willett, shengli} @engr.uconn.edu).

1557-6418/14/$17.00

I. INTRODUCTION

Passive Bistatic Radar (PBR), also known as Passive Coherent Location (PCL), uses illuminators of opportunity. Passive radar using signals in a single frequency network modulated according to the Digital Audio/Video Broadcasting (DAB/DVB) standards using orthogonal frequency division multiplexing (OFDM) has recently been of increasing interest. There has been considerable research to develop tracking systems addressing its inherent difficulties [3]–[7], [10]–[13]; the poor quality—or absence—of angular information, and the lack of label of the transmitter on top of the usual target/measurement association concerns.

First, there are algorithms using the Multi-Hypothesis Tracker (MHT) [12], [13] addressing the complexity problem from association ambiguities between measurement, targets and illuminators by initially forming two dimensional (measurement-target) hypotheses in the two-dimensional range/Doppler domain. Tracking is thence performed directly on target parameters by the MHT without considering the association between measurements and illuminators: the range/Doppler MHT extracts measurements and removes false alarms. Then, de-ghosting is performed by evaluating likelihood probabilities of possible data associations. When a Cartesian track is confirmed, the remaining tracks from other possible associations are declared false and tracking starts in the Cartesian domain.

This MHT approach is good but but is not without issues. One is the appropriate motion model in range and Doppler space: probably the target dynamics in the Cartesian domain are known, the trajectories are not easily described in a space of target parameters, because the trajectories are related to illuminator/receiver/target geometry and there is association ambiguity among measurements, illuminators, and targets. And that is another concern: the illuminator association is never explicitly addressed.

Now, track maintenance algorithms that operate directly in Cartesian coordinates have been explored [4], [5], one using modified Joint Probabilistic Data Association (JPDA) and another a particle filter. For the former, in order to address the large number of three-list hypotheses, a "super-target" idea was proposed; and the particle filters work under the PMHT measurement model that each measurement's assignments are independent of others'. These methods have also been examined downstream from an initiation approach (the PMHTI method, suggested in [6]) that initiates tracks in Cartesian coordinates.

In fact the PMHT seems to be an effective and natural way to accommodate the data association with the extra list (transmitters). So in this paper, we present it: it is really very simple. This tracker, combined with the initiation algorithm (the modified PMHTI method in [6]), shows excellent performance in comparison with the JPDA filter and particle filter.

Section II explains what tracking in the Cartesian domain involves. Section III presents the PMHT solution, as well as a brief summary of the modified initiation algorithm. There are results in Section IV. We wish to note that although the motivating example is DAB/DVB passive radar, the techniques here could apply to any multistatic system (e.g., sonar) with common transmitter waveform. The common key ingredient is the measurements' lack of illuminator label.

II. MODEL

A. Process

We assume that there are multiple targets. For the mth target the state

$$\mathbf{x}_m(t_i) = [x_m(t_i), \dot{x}_m(t_i), y_m(t_i), \dot{y}_m(t_i), z_m(t_i), \dot{z}_m(t_i)]$$

is to be estimated, and comprises its location $\mathbf{p}_m(t_i) = [x_m(t_i), y_m(t_i), z_m(t_i)]^T$ and velocity $\mathbf{v}_m(t_i) = [\dot{x}_m(t_i), \dot{y}_m(t_i), \dot{z}_m(t_i)]^T$.

Each target moves according to a model that makes sense in the Cartesian[1] domain, such as according to kinematic dynamics or constant-speed turn. We assume there are M_{t_i} targets at time t_i, such that the goal is to estimate $\{\{\mathbf{x}_m(t_i)\}_{m=1}^{M_{t_i}}\}_{i=1}^{T}$. Track management (determination of M_{t_i}) is not the subject of this correspondence; however, we suggest the techniques of [6] for initiation (the more difficult component) and we later give some suggestions for termination. We do not address track-merging or -spawn.

There are N_s illuminators, the sth being located at $\mathbf{x}_s = [x_s, y_s, z_s]^T$; and there is assumed a single receiver at $\mathbf{x}_r = [x_r, y_r, z_r]^T$. The receiver can for target m measure bistatic range $\gamma(t_i)$ and range-rate $\dot{\gamma}(t_i)$, which are given by

$$\gamma(\mathbf{x}_m(t_i), \mathbf{x}_s) = \|\mathbf{p}_m(t_i) - \mathbf{x}_r\| + \|\mathbf{p}_m(t_i) - \mathbf{x}_s\| \tag{1}$$

$$\dot{\gamma}(\mathbf{x}_m(t_i), \mathbf{x}_s) = \frac{(\mathbf{p}_m(t_i) - \mathbf{x}_r)^T \cdot \mathbf{v}_m(t_i)}{\|\mathbf{p}_m(t_i) - \mathbf{x}_r\|} + \frac{(\mathbf{p}_m(t_i) - \mathbf{x}_s)^T \cdot \mathbf{v}_m(t_i)}{\|\mathbf{p}_m(t_i) - \mathbf{x}_s\|} \tag{2}$$

in which $s \in \{1, \ldots, N_s\}$. The generic observation vector in the absence of noise is given by

$$h_s(\mathbf{x}(t_i)) = (\gamma(\mathbf{x}(t_i), \mathbf{x}_s), \dot{\gamma}(\mathbf{x}(t_i), \mathbf{x}_s))^T. \tag{3}$$

Hence, the measurement at time t_i for target m and involving illuminator s is

$$z(t_i) = h_s(\mathbf{x}_m(t_i)) + \nu_{m,s}(t_i) \tag{4}$$

with $\nu_{m,s}(t_i)$ independent, zero-mean and Gaussian measurement noises of covariance $R_{m,s}(t_i)$.

While (4) is a function of the target $\mathbf{x}_m(t_i)$ and transmitter $\mathbf{x}_s$, the observations available to the tracker at time t consist of a set $\{z^{(r)}(t_i)\}$ with components unlabeled as to m nor s—the uncertainty as to the transmitter s is a new visitor to the usual "measurement-origin uncertainty" (MOU) model. On the other hand, a familiar ingredient to MOU is that although all combinations of s and m (that is: $N_s \times M$ elements) might be thought an "original" set of measurements, but these are thinned according to a Bernoulli process: each is retained with probability P_d and else discarded. Another familiar ingredient is that the set of survivors be augmented by a Poisson set of false alarms uniformly distributed in range & range-rate.

The PMHT model [8], [16], [19] is different, and will be described in detail in the next section. However, its features are:

- that the model is not *generative*: that is, it is posterior to knowing the number of measurements available;
- that the a priori association probabilities (of each measurement having arisen from target m and due to transmitter s) are independent for each measurement; and
- that each target/transmitter pair be represented at most once per time t_i in the observation set is not enforced;

The model is not reflective of our passive-radar physics; however, it is clear and unashamed, and it results in a feasible algorithm that works quite effectively.

III. THE PMHT

A. Description of the algorithm

When there are N_s illuminators[2] and M targets, at each measurement time t_i ($i = 1, 2, \ldots, T$), a state of target m is denoted by $\mathbf{x}_m(t_i)$. X_T is the collection of states for all targets up to time T and Z_T is the set of conditionally statistically independent measurements, in which $Z_T = (Z_{t_0}, Z_{t_1}, \ldots, Z_{t_T})$, where $Z_{t_i} = (\mathbf{z}_{t_i}^{(1)}, \mathbf{z}_{t_i}^{(2)}, \ldots, \mathbf{z}_{t_i}^{(N_{t_i})})$—there are N_{t_i} measurements at time t_i. In fact, we have:

- The statistically independent measurement-to-target assignments are described by $\mathcal{K}_T = (\mathcal{K}_{t_0}, \mathcal{K}_{t_1}, \ldots, \mathcal{K}_{t_T})$ and $\mathcal{K}_{t_i} = (k_{t_i}^{(1)}, k_{t_i}^{(2)}, \ldots, k_{t_i}^{(N_{t_i})})$ where $1 \leq k_{t_i}^{(r)} \leq M$ denotes the index of the target assigned to the measurement $z_{t_i}^{(r)}$.
- The (again: statistically independent) measurement-to-illuminator assignments—the new illuminator-to-measurement association ambiguity—are denoted $\mathcal{L}_T = (\mathcal{L}_{t_0}, \mathcal{L}_{t_1}, \ldots, \mathcal{L}_{t_T})$, in which $\mathcal{L}_{t_i} = (l_{t_i}^{(1)}, l_{t_i}^{(2)}, \ldots, l_{t_i}^{(N_{t_i})})$ and $1 \leq l_{t_i}^{(r)} \leq N_s$ is the index of illuminator assigned to the measurement $\mathbf{z}_{t_i}^{(r)}$.

The "usual" PMHT association model accommodates more than one measurement being assigned to each target, and that remains so here. But note also that each target can further be associated with more than one measurement for each illuminator. Physically this is wrong; algorithmically it is a nice feature.

[1] Since these models are well known, this short paper simply defers to references, for example [1].

[2] We use the subscript s mostly to avoid confusion, but defensibly to indicate the ground-station in the DVB/DAB network.

In the usual case having only one kind of data association ambiguities between measurements and targets, the PMHT uses the EM algorithm to maximize $p(X_T \mid Z_T)$ over X_T [8], [9], [19], utilizing the quantity

$$Q(X_T^{(n+1)} \mid X_T^{(n)}) \equiv \sum_{\mathcal{K}_T} \ln(p(X_T^{(n+1)}, \mathcal{K}_T \mid Z_T)) p(\mathcal{K}_T \mid X_T^{(n)}, Z_T), \quad (5)$$

instead of directly finding the MAP (maximum a posteriori) estimate of X_T

$$X_{\text{MAP}} = \arg\max_{X_T} E\{\ln(p(X_T \mid Z_T))\}. \quad (6)$$

At each iteration, the algorithm finds

$$X_T^{(n+1)} = \arg\max_{X_T^{(n+1)}} Q(X_T^{(n+1)} \mid X_T^{(n)}) \quad (7)$$

achieving $p(X_T^{(n+1)} \mid Z_T) > p(X_T^{(n)} \mid Z_T)$.

Generalizing this to the case having the additional association ambiguities between measurements and illuminators, the quantity $Q(X_T^{(n+1)} \mid X_T^{(n)})$ is

$$Q(X_T^{(n+1)} \mid X_T^{(n)}) \equiv \sum_{\mathcal{K}_T, \mathcal{L}_T} \ln(p(X_T^{(n+1)}, \mathcal{K}_T, \mathcal{L}_T \mid Z_T)) \times p(\mathcal{K}_T, \mathcal{L}_T \mid X_T^{(n)}, Z_T). \quad (8)$$

Assuming $P(k_{t_i}^{(r)} = m) = \pi_m^k$ and $P(l_{t_i}^{(r)} = s) = \pi_s^l$, the conditional pdf for all measurements is as follows:

$$P(\mathcal{K}_T, \mathcal{L}_T \mid X_T^{(n)}, Z_T) = \prod_{i=1}^{T} \prod_{r=1}^{N_{t_i}} \omega_{t_i,r}^{(n)}(m,s) \quad (9)$$

in which

$$\omega_{t_i,r}^{(n)}(m,s) = \frac{\pi_m^k \pi_s^l p(\mathbf{z}_{t_i}^{(r)} \mid k_{t_i}^{(r)} = m, l_{t_i}^{(r)} = s, \mathbf{x}_m^{(n)}(t_i))}{\sum_{p=1}^{M} \sum_{q=1}^{N_s} \pi_p^k \pi_q^l p(\mathbf{z}_{t_i}^{(r)} \mid k_{t_i}^{(r)} = p, l_{t_i}^{(r)} = q, \mathbf{x}_p^{(n)}(t_i))}. \quad (10)$$

It is noted that $\omega_{t_i,r}^{(n)}(m,s)$ denotes the posterior probability of measurement r being related to target m and illuminator s at time t_i at the nth EM iteration.

Now, we have

$$Q(X_T^{(n+1)} \mid X_T^{(n)}) = \sum_{\mathcal{K},\mathcal{L}} \ln[p(X^{(n+1)}, \mathcal{K}, \mathcal{L}, Z_T) p(\mathcal{K}, \mathcal{L} \mid X^{(n)}, Z_T)] \quad (11)$$

$$= \ln\left[\prod_{q=1}^{M} (p(\mathbf{x}_q^{(n+1)}(t_1)) \prod_{i=2}^{T} p(\mathbf{x}_q^{(n+1)}(t_i) \mid \mathbf{x}_q^{(n+1)}(t_{i-1}))\right] \quad (12)$$

$$+ \sum_{m=1}^{M_t} \sum_{s=1}^{N_s} \sum_{i=1}^{T} \sum_{r=1}^{N_{t_i}} (\omega_{t_i,r}^{(n)}(m,s) \ln[\pi_m^k \pi_s^l] + \omega_{t_i,r}^{(n)}(m,s) \ln[p(\mathbf{z}_{t_i}^{(r)} \mid k_{t_i}^{(r)} = m, l_{t_i}^{(r)} = s, \mathbf{x}_m^{(n+1)}(t_i))])$$

so

$$\nabla_{X^{(n+1)}} Q(X^{(n+1)} \mid X^{(n)}) = \nabla_{X^{(n+1)}} \left[\ln\left[\prod_{q=1}^{M} (P(\mathbf{x}_q^{(n+1)}(t_1)) \times \prod_{i=2}^{T} P(\mathbf{x}_q^{(n+1)}(t_i) \mid \mathbf{x}_q^{(n+1)}(t_{i-1}))\right]\right] + \sum_{m,s} \sum_{i=1}^{T} \nabla_{X^{(n+1)}} h_s(\mathbf{x}_m^{(n+1)}(t_i)) \times \left[\left(\frac{R_{m,s}(t_i)}{\sum_{r=1}^{N_{t_i}} \omega_{t_i,r}^{(n)}(m,s)}\right)^{-1} \times \left(\sum_{r=1}^{N_{t_i}} \frac{\omega_{t_i,r}^{(n)}(m,s)(\mathbf{z}_{t_i}^{(r)})}{\sum_{r=1}^{N_{t_i}} \omega_{t_i,r}^{(n)}(m,s)} - h_s(\mathbf{x}_m^{(n+1)}(t_i))\right)\right] \quad (13)$$

Similar to [19], $\nabla_{X_T^{(n+1)}} Q(X_T^{(n+1)} \mid X_T^{(n)})$ is equal to the gradient of logarithm of the joint "synthetic" Q-function $\tilde{Q}(X_T^{(n+1)} \mid X_T^{(n)})$ having no data association uncertainty with synthetic measurement $\tilde{\mathbf{z}}_{m,s}$ and synthetic measurement covariance $\tilde{R}_{m,s}(t_i)$. That is, we have

$$\nabla_{X^{(n+1)}} Q(X_T^{(n+1)} \mid X_T^{(n)}) = \nabla_{X_T^{(n+1)}} \tilde{Q}(X_T^{(n+1)} \mid X_T^{(n)}) \quad (14)$$

where

$$\tilde{Q}(X_T^{(n+1)} \mid X_T^{(n)}) = \ln\left[\prod_{q=1}^{M} (p(\mathbf{x}_q^{(n+1)}(t_1)) \prod_{i=2}^{T} p(\mathbf{x}_q^{(n+1)}(t_i) \mid \mathbf{x}_q^{(n+1)}(t_i - 1))\right] - \frac{1}{2} \sum_{m=1}^{M_t} \sum_{s=1}^{N_s} \sum_{i=1}^{T} [\tilde{\mathbf{z}}_{t_i}(m,s) - h_s(\mathbf{x}_m^{(n+1)}(t_i))]^T \times \tilde{R}_{m,s}(t_i)^{-1} [\tilde{\mathbf{z}}_{t_i}(m,s) - h_s(\mathbf{x}_m^{(n+1)}(t_i))], \quad (15)$$

we obtain

$$\tilde{\mathbf{z}}_{m,s}(t_i) = \frac{\sum_{r=1}^{N_{t_i}} \omega_{t_i,r}^{(n)}(m,s) \mathbf{z}_{t_i}^{(r)}}{\sum_{r=1}^{N_{t_i}} \omega_{t_i,r}^{(n)}(m,s)} \quad (16)$$

$$\tilde{R}_{m,s}(t_i) = \frac{R_{m,s}(t_i)}{\sum_{r=1}^{N_{t_i}} \omega_{t_i,r}^{(n)}(m,s)} \quad (17)$$

The form of (15) reflects the nonlinearity of the measurement model (4) by involving $h_s(\mathbf{x}_m^{(n+1)}(t_i))$ explicitly. If one's taste leans towards the unscented Kalman filter (UKF) (e.g., [2]) this is useful. Perhaps it is more familiar to write

$$H_{m,s}(t_i) = \nabla_{X^{(n)}} h_s(\mathbf{x}_m^{(n)}(t_i)) \quad (18)$$

suggesting that an extended Kalman filter (EKF) [1] can be used within a Kalman smoother.

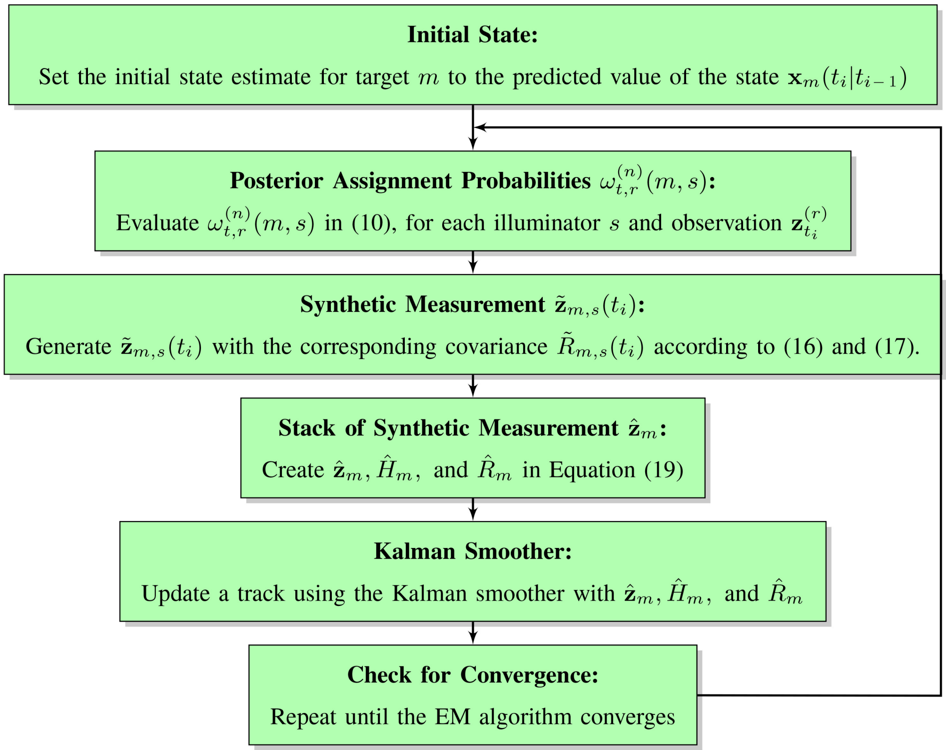

Fig. 1. PMHT (tracking) algorithm to update the state and covariance of target m at time t_i. If an EKF is used, $\tilde{\mathbf{z}}_{m,s}(t_i)$ in the third step should be replaced by $\tilde{\mathbf{z}}_{m,s}(t_i) - [h_s(\mathbf{x}_m^{(n)}(t_i)) - H_{m,s}(t_i)\mathbf{x}_m^{(n)}(t_i)]$.

That is, an iterated (extended) Kalman smoother routine using "synthetic" measurements $\{\tilde{\mathbf{z}}_{m,s}(t_i)\}_{i=1}^T$ and corresponding covariances $\{\tilde{R}_{m,s}(t_i)\}_{i=1}^T$ from (16) and (17) for each target m would be sufficient if there were only one transmitter $s = N_s = 1$, although a full Cartesian track would problematic if there were only one transmitter. To exploit the multi-sensor "triangulation" necessary for Cartesian tracking it is necessary to fuse data from multiple illuminators. There are various methods [8], [14], [15], [17] for this, and we adopt here that using stacked synthetic measurements:

$$\hat{\mathbf{z}}_m(t_i) = [\tilde{\mathbf{z}}_{m,1}^T(t_i), \tilde{\mathbf{z}}_{m,2}^T(t_i), \ldots, \tilde{\mathbf{z}}_{m,N_s}^T(t_i)]^T \tag{19}$$

$$\hat{H}_m(t_i) = \mathrm{diag}[H_{m,1}(t_i), H_{m,2}(t_i), \ldots, H_{m,N_s}(t_i)]$$

$$\hat{R}_m(t_i) = \mathrm{diag}[\tilde{R}_{m,1}(t_i), \tilde{R}_{m,2}(t_i), \ldots, \tilde{R}_{m,N_s}(t_i)]$$

The algorithm is described in Figure 1. We note that the PMHT is known sometimes to converge to a local MAP (basically a lost track) [19]. In our study here we have not suppressed this behavior; but it seems to be a lesser problem for the PMHT than the additional data association that vexes the other approaches.

In the following section we will compare this new method to the modified JPDA and particle filter (PF) approaches. Hence in the next two subsections we will mention the track-management schemes used for this comparison.

B. Initiation of tracks

To initiate tracks, we adopt the PMHTI method presented in [6]. To decrease complexity caused by the search for local maxima of $p(Z \mid \mathbf{p})$ using *all* the points obtained by the spherical-intersection method, we modify the search step to use only the initialization points having the highest likelihoods (rather than all the points). We call this the modified PMHTI method in Figure 2.

Here, a track is confirmed in the PMHT if the sum of measurement weights is higher than a certain threshold for three out of five consecutive scans, and the estimated covariance is smaller than a certain threshold. The JPDA filter confirms a track if there is at least one measurement within the target's gate for three out of five consecutive scans and the gate is smaller than a certain threshold. The particle filter confirms temporary tracks if there is at least one measurement in the validation region for three out of five consecutive scans.

C. Track Termination

Respectively, these use:

1) PMHT: In the PMHT, a track is called lost if the sum of weights of measurements (i.e., $\sum_s \omega_{t_i,r}^{(n)}(m,s)$) is less than a certain threshold for three out of five consecutive scans, or the estimated covariance is larger than a certain threshold.

2) JPDA using the Extend Kalman filter: The track is declared lost if no measurement falls within the

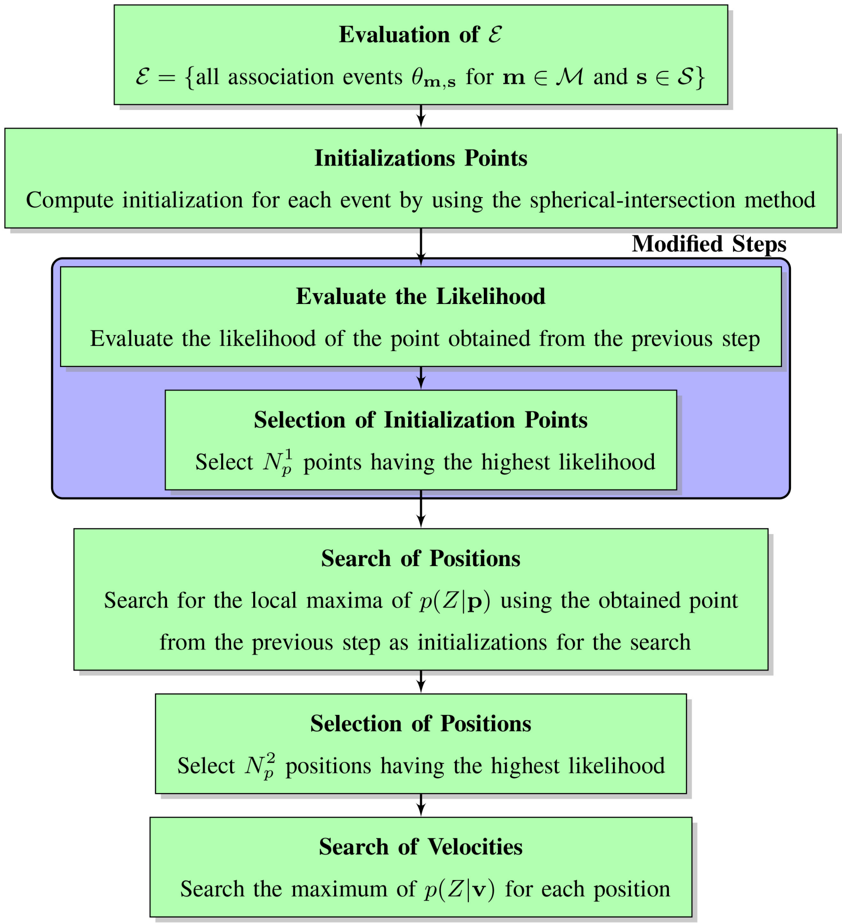

Fig. 2. Modified PMHTI (initiation) method: $\mathcal{M}$ is a set of 3-permutations of measurements and $\mathcal{S}$ is a set of 3-combinations of illuminators. N_p^1 and N_p^2 are thresholds, and the position and velocity is denoted by $\mathbf{p}$ and $\mathbf{v}$, respectively.

target's gate [2] for three out of five consecutive scans or the gate is larger than a certain threshold. When the predicted measurement $\hat{\mathbf{z}}$ and the associated covariance S are given, the measurement $\mathbf{z}$ is considered to be in the validation region if $(\mathbf{z} - \hat{\mathbf{z}})^T S^{-1}(\mathbf{z} - \hat{\mathbf{z}}) < \gamma$, where the threshold γ denotes the gate size.

3) PF: The particle filter defines the validation region by using statistical distance in measurement space [2], [18]: when $\hat{\mathbf{z}}$ is the converted measurement from an estimated state and R is the measurement noise covariance, the measurement $\mathbf{z}$ is defined as valid if $(\mathbf{z} - \hat{\mathbf{z}})^T R^{-1}(\mathbf{z} - \hat{\mathbf{z}}) < \gamma$ for threshold γ. If there is no measurement in the validation region for three out of five consecutive scans, or every particle has negligible weight caused by impoverishment/degeneracy of particles, the track is declared lost. It is noted that the particle filter does not use the validation region to estimate the state, unlike the JPDA.

IV. SIMULATION

It is assumed that there are three targets, five illuminators and one receiver, as in Figure 3. False measurements are uniformly distributed with spatial density λ in a surveillance region of volume V in range-/range-rate space, while their number ϕ is Poisson. The measurement noise follows a Gaussian distribution $\mathcal{N}(0, \sigma_\gamma^2)$ for range, and $\mathcal{N}(0, \sigma_{\dot{\gamma}}^2)$ for range-rate. 100 Monte Carlo runs are performed and 2,000 particles are used in the particle filter. Track management is integral to the simulation: no tracker has prior information as to the number of targets. For the initiation method $N_p^1 = 50$ and $N_p^2 = 3$ are chosen (see Figure 2). The PMHT uses a sliding batch (see [19]) of length 5.

A. Comparison in Terms of Target Number

We compare the PMHT to the modified JPDA filter and the (bootstrap) particle filter [5], where in each case the PMHTI method [6] is used for track initiation and using track confirmation/termination as described earlier. Trajectories from the previous simulation (pictured in Figure 3) are used, but they begin at different times and last for fewer than 60 scans in order to examine the performance of track management. In this subsection, the measurement noise standard deviation is $\sigma_\gamma = 20$ m and $\sigma_{\dot{\gamma}} = 2$ m/s.

The PMHT filter confirms and terminates tracks remarkably well, regardless of the false alarm density and the detection probability, as seen in Figures 4 and

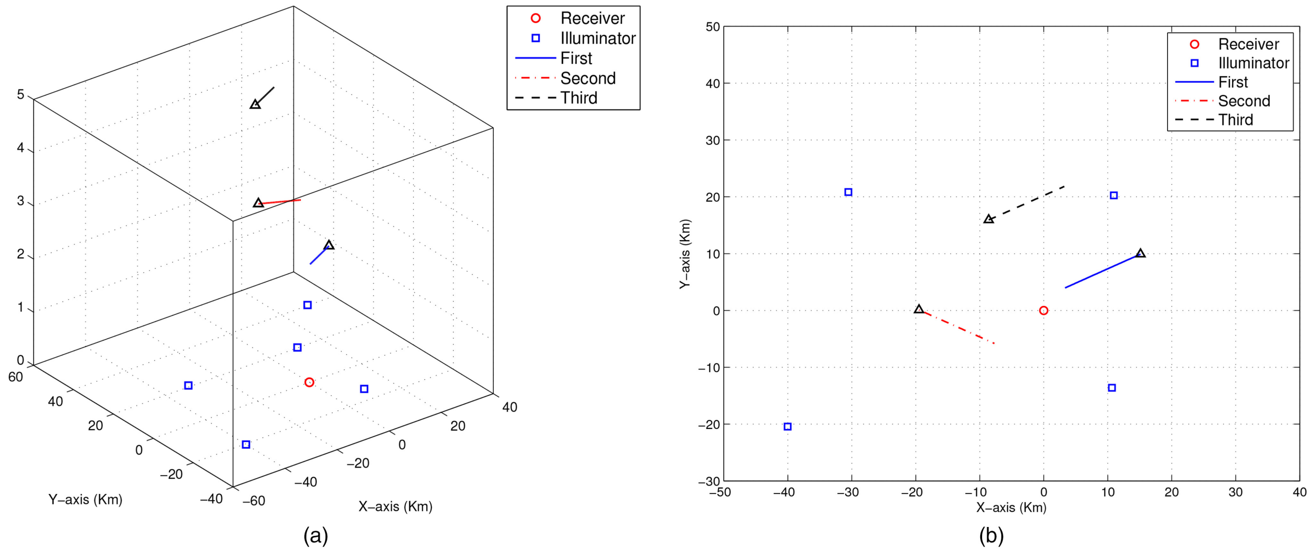

Fig. 3. Trajectories with three targets, five illuminators and one receiver. (a) Three dimensional space. (b) Projected in a two dimensional space.

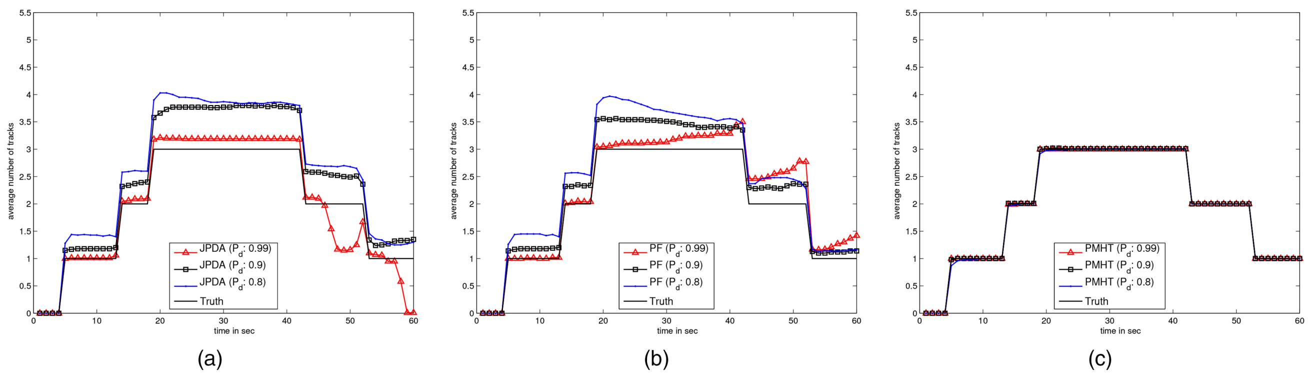

Fig. 4. Average number of confirmed tracks with low false alarm density ($\lambda V = 1$): the PMHT almost overlaps with the ground truth. (a) JPDAF. (b) Particle Filter. (c) PMHT.

6, where the performance almost does not degrade for the high false alarm density. Although the JPDA and particle filters show good performance with a low false alarm density, when the expected number of false alarms is increased to four the termination of tracks in the JPDA filter degrades (track confirmation is still quite good) and the particle filter deteriorates according to both measures.

As expected, the number of temporary tracks in every tracker increases at higher false alarm rates, as seen in Figures 5 and 7. It is also shown that this number is strongly related to the number of confirmed tracks. For example, since the particle filter does not perform termination and confirmation especially well in high clutter, there are more confirmed tracks and fewer temporary ones compared to the other trackers in Figures 6 and 7, since if more measurements are within the validation region of the confirmed tracks there are fewer measurements to initiate temporary tracks.

It is noted that the modifications to the termination rule affect track confirmation, for example a stricter termination rule could terminate temporary tracks too easily before they are confirmed. When stricter termination and confirmation rules are applied to these filters (e.g., two out of seven scans for termination and five out of seven scans for confirmation), the performance of the JPDA filter is severely degraded and the particle filter's performance is also worsened, especially at lower detection probabilities. In the PMHT filter, the threshold on the sum of the weights is more influential on the performance than the choice of termination/confirmation rules and the appropriate threshold is also critical to show the good performance.

We also note that in this simulation the PMHT, with its simplified data association, does not require many iterations to converge; while the JPDAF still needs to evaluate all data association events and the particle filter must update every particle's weight. Hence, at least in our experience, the PMHT is considerably faster than the JPDA and particle filter approaches.

B. Comparison in Terms of Track Accuracy

We have carried out additional comparison of the trackers via RMSE. In order to remove the effect of

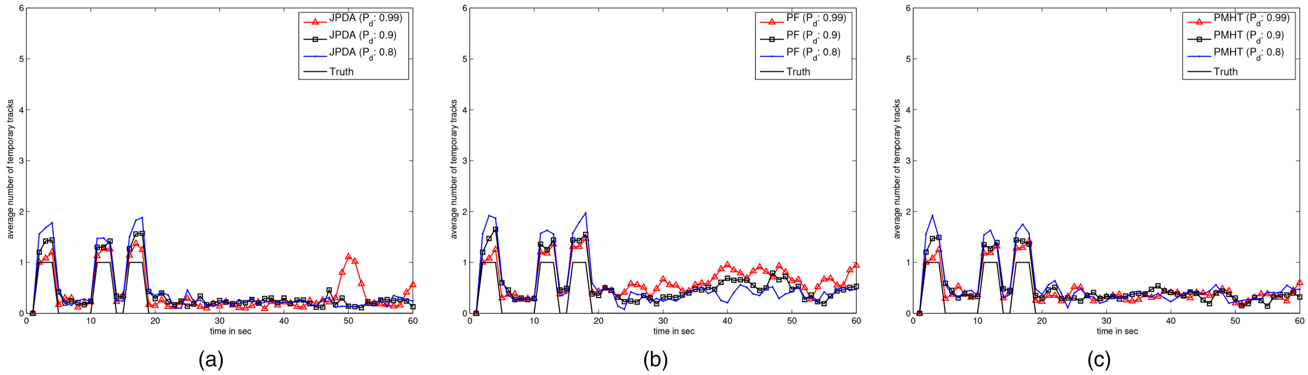

Fig. 5. Average number of temporary tracks with the low false alarm density ($\lambda V = 1$): the truth is the number of true tracks considered as temporary tracks following the track confirmation rule. (a) JPDAF. (b) Particle Filter. (c) PMHT.

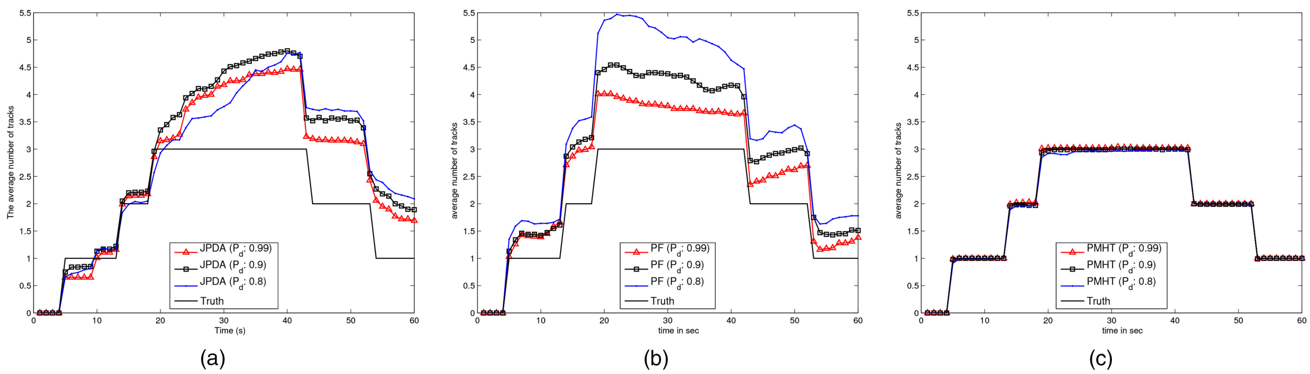

Fig. 6. Average number of confirmed tracks with high false alarm density ($\lambda V = 4$): the PMHT shows similar performance to the case having low false alarm density, unlike other filters. (a) JPDAF. (b) Particle Filter. (c) PMHT.

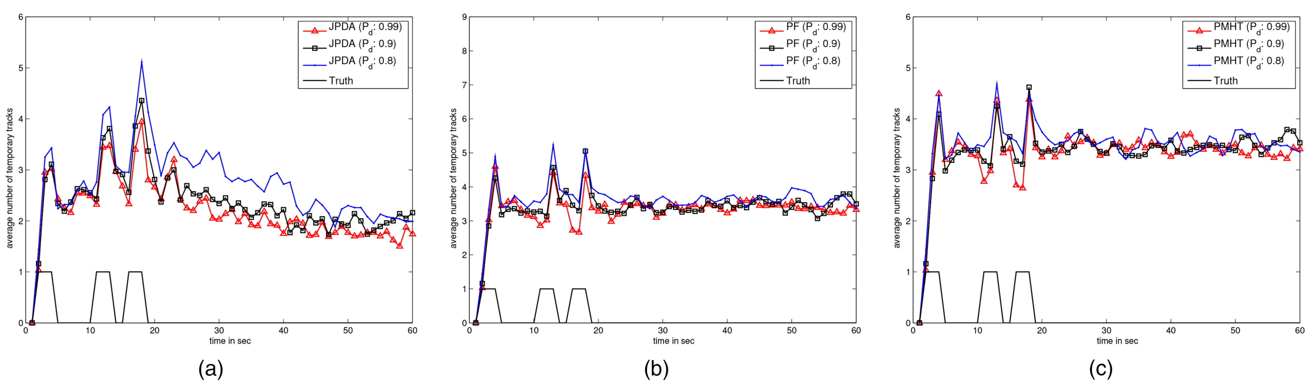

Fig. 7. Average number of temporary tracks with high false alarm density ($\lambda V = 4$): the truth is the number of true tracks considered as temporary tracks following the track confirmation rule. Due to the high false alarm density, the number of temporary tracks apparently increases. (a) JPDAF. (b) Particle Filter. (c) PMHT.

the initiation algorithm, the initial $\mathbf{p}$ and velocity $\mathbf{v}$ are generated from the position $\mathbf{p}_0$ and velocity $\mathbf{v}_0$ of ground truth such that $\mathbf{p} = \mathbf{p}_0 + \omega_1$ and $\mathbf{v} = \mathbf{v}_0 + \omega_2$, where ω_i follows Gaussian distribution $\mathcal{N}(0, \sigma_i^2)$ with $\sigma_1 = \sigma_\gamma$ and $\sigma_2 = 2\sigma_{\dot{\gamma}}$.

For the measurement noise of $\sigma_\gamma = 20$ m and $\sigma_{\dot{\gamma}} = 2$ m/s, the RMSE of the PMHT decreases over time, while the other filters show the opposite tendency (with the exception of the JPDA filter with $P_d = 0.7$), as seen in Figures 8 and 9; presumably this follows from the PMHT's batch-optimization behavior. The performance of the PMHT filter was found to be more sensitive to the illuminator/receiver/target geometry than the other filters. At this level of measurement noise, there was no lost track. It is also noted that the RMSE of the second target is very similar to the third target and is not shown here.

When the range measurement noise is increased to $\sigma_\gamma = 100$ m, the performance of the PMHT for the third target is a little worse than the case having the low measurement noise, but the RMSE of PMHT for the first target with the low detection probability ($P_d = 0.7$)

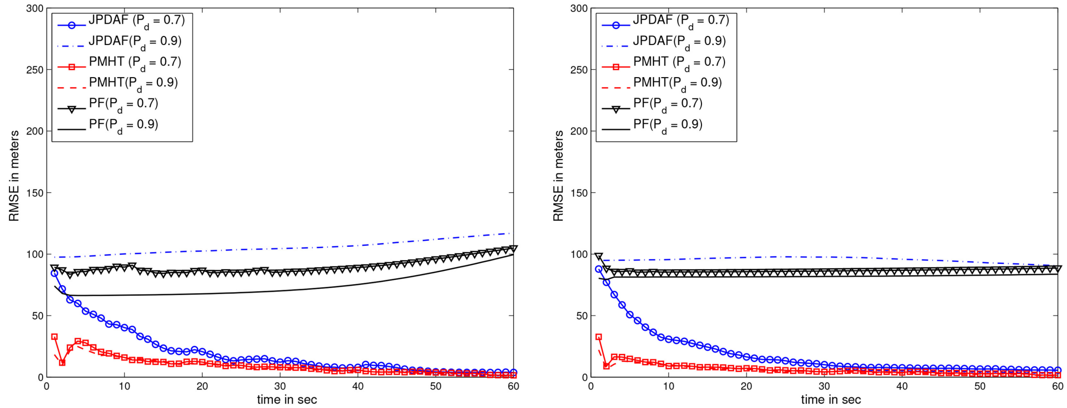

(a) (b)

Fig. 8. RMSE for different detection probabilities with $\lambda V = 1$ and low measurement noise ($\sigma_\gamma = 20$ m and $\sigma_{\dot{\gamma}} = 2$ m/s): the RMSE is less than 150 m, and the RMSE of the PMHT decreases while the other filters increase, but it is sensitive to illuminator/receiver/target geometry. (a) First Target. (b) Third Target.

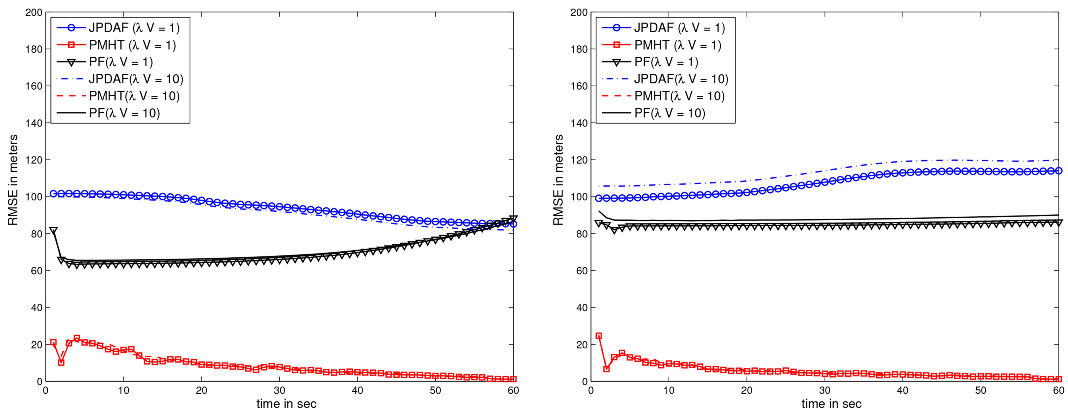

(a) (b)

Fig. 9. RMSE for different expected numbers of false alarms (λV) with detection probability $P_d = 0.99$ and low measurement noise ($\sigma_\gamma = 20$ m and $\sigma_{\dot{\gamma}} = 2$ m/s): the RMSE is less than 180 m and the high false alarm rate has a more profound effect on the PMHT than the low detection probability. (a) First Target. (b) Third Target.

or the high expected number of false alarm ($\lambda V = 10$) is clearly degraded more than other filters, as seen in Figures 10 and 11. The tendency of the RMSE to decrease over time for the PMHT is still present in this case. The rate of track loss in the PMHT filter is less than 2% with detection probability less than 0.8, while there is no lost track in the JPDA filter for every case. The track loss in the particle filter reaches 30% when the detection probability is 0.7. Additionally, the JPDA filter's performance with the low detection probability is better than the high detection probability as seen in Figures 8 and 10, meaning that many measurements degrade the data association rather than help. Further, the performance of the JPDA filter seems unaffected by a higher false alarm density, as seen in Figures 9 and 11. We note that tracker RMSE curves vary significantly with geometry and other factors [5].

C. Discussion

There are separate results for comparisons in terms of track management and in terms of track accuracy. The former are clear and depend little on geometry nor parameter settings: the PMHT is remarkably accurate at determining the number of extant tracks. We have shown typical examples of the latter that strongly imply considerable preferability of the PMHT. But these results depend more on geometry and parameter settings, and it can be difficult to distinguish a track that is being lost from one that is merely bad. Nonetheless, on the basis of these results and others—and also on our observation of computational needs—we confidently contend that the PMHT approach (coupled with the PMHTI for track initiation and simple rules for validation and termination) is the way to go.

It is harder to be confident as to why. We offer the following. All three of these algorithms are approximations. The "super-targets" in the JPDAF's association model are a convenience (plus its "memory" is only one scan); the PMHT uses an "incorrect" assignment prior; and the particle filter both uses a form of the PMHT model and becomes exact only in the limit as the number of particles diverges. It seems that the PMHT's price (modeling) is worth the benefit (multiscan operation).

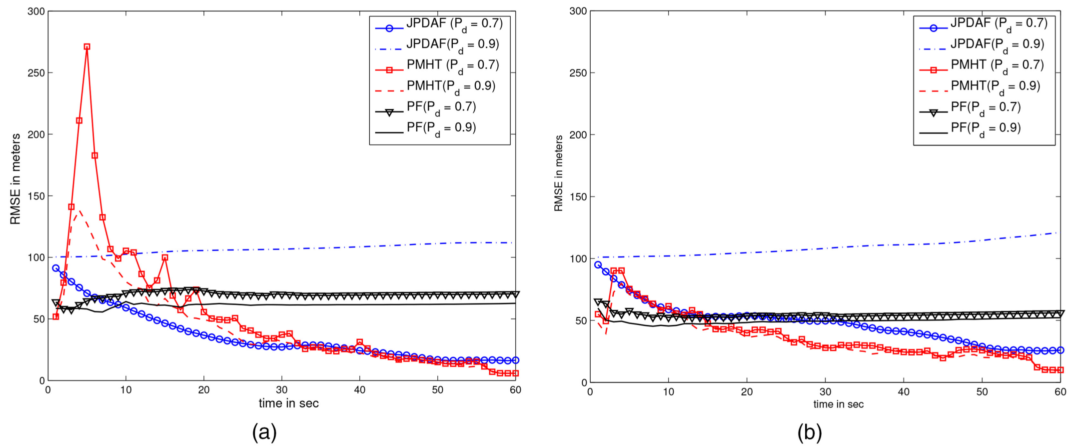

Fig. 10. RMSE for different detection probabilities with high measurement noise (σ_{γ} = 100 m and $\sigma_{\dot{\gamma}}$ = 2 m/s): the RMSE is less than 1,000 m. (a) First Target. (b) Third Target.

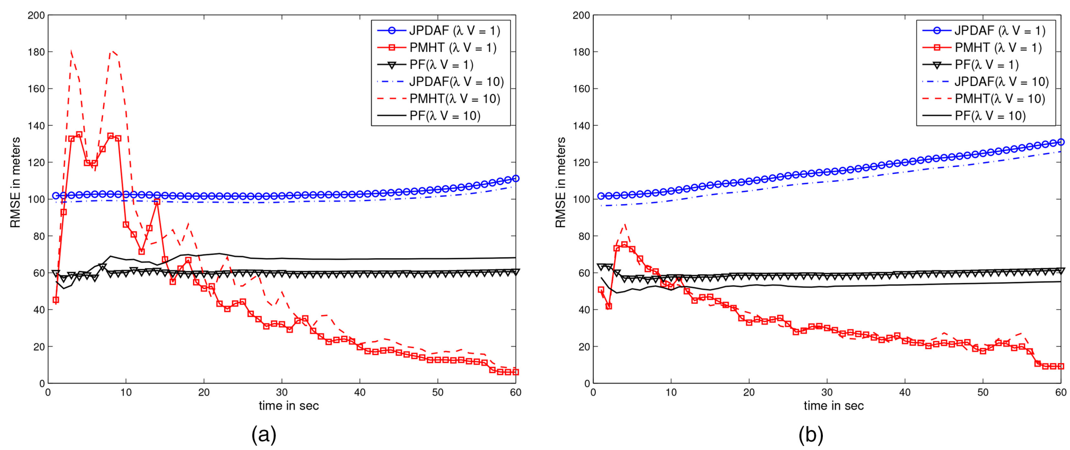

Fig. 11. RMSE for different expected numbers of false alarm (λV) with high measurement noise (σ_{γ} = 100 m and $\sigma_{\dot{\gamma}}$ = 2 m/s): the RMSE is less than 1,400 m, and the PMHT filter is more affected by the high false alarm density than other filters. (a) First Target. (b) Third Target.

V. SUMMARY

The design of a passive radar system poaching DAB/DVB signals is challenging, due both to the poor quality of angular information and to the use of indistinguishable signals from multistatic transmitters—there is an additional association ambiguity between measurements and illuminators. A tracking system using the PMHT to deal with the measurement-illuminator-target association was here presented. This (modified) PMHT was compared with a modified JPDA filter and particle filter. When these trackers are combined with the PMHTI method for track-initiation, the PMHT shows excellent performance compared to the other filters. In terms of computational complexity, the PMHT filter is in our experience faster as well.

REFERENCES

[1] Y. Bar-Shalom, X.-R. Li, and T. Kirubarajan.
Estimation with Application to Tracking and Navigation.
YBS publishing, Storrs, CT, 1995.

[2] Y. Bar-Shalom, P. Willett, and X. Tian.
Tracking and Data Fusion: A Handbook of Algorithms.
YBS Publishing, Storrs, CT, 2011.

[3] C. Berger, B. Demissie, J. Heckenbach, P. Willett, and S. Zhou.
Signal processing for passive radar using OFDM waveforms.
IEEE Journal on Selected Topics in Signal Processing (special issue on MIMO Radar), 10(5):226–238, 2010.

[4] S. Choi, C. Berger, D. Crouse, P. Willett, and S. Zhou.
Target tracking for multistatic radar with transmitter uncertainty.
In *Proceedings of SPIE:Signal and Data Processing of Small Targets 2009*, volume 7445, 2009.

[5] S. Choi, D. Crouse, P. Willett, and S. Zhou.
Approaches to Cartesian data association passive radar tracking in a DAB/DVB network.
available at the *IEEE Trans. on Aerospace and Electronic Systems*, page doi:10.1117/12.829599.

[6] S. Choi, D. Crouse, P. Willett, and S. Zhou.
Multistatic target tracking for passive radar in a DAB/DVB network: Initiation.
submitted in the *IEEE Trans. on Aerospace and Electronic Systems*.

[7] D. Crouse.
A time-shift model for OFDM radar.
In *The 2012 IEEE Radar Conference*, pages 841–846, Washington, DC, 2012.

[8] D. Crouse, M. Guerriero, and P. Willett.
A critical look at the PMHT.
Journal of Advances in Information Fusion, 4(2):93–116, December 2009.

[9] D. Crouse, M. Guerriero, P. Willett, R. Streit, and D. Dunham. A look at the PMHT. In *Proc. of the 12th International conference on Information Fusion*, pages 332–339, Seattle, WA, 2009.

[10] M. Daun and C. Berger. Track initialization in a multistatic DAB/DVB-T network. In *Proceeding of the 11th International Conference on Information Fusion*, Cologne (Germany), July 2008.

[11] M. Daun and R. Kaune. Gaussian mixture initilization in passive tracking applications. In *Information Fusion, 2010 13th Conference on*, pages 1–8, Rome, Italy, July 2010.

[12] M. Daun and W. Koch. Multistatic target tracking for non-cooperative illumination by DAB/DVB-T. In *IEEE Radar Conference*, page DIO 4302238, Rome, Italy, May 2008.

[13] M. Daun, U. Nickel, and W. Koch. Tracking in multistatic passive radar system using DAB/DVB-T illumination. *Signal Processing*, 92(6):1365–1386, June 2012.

[14] E. Giannopoulos, R. Streit, and P. Swaszek. Probabilistic multi-hypothesis tracking in a multi-sensor, multi-target environment. In *Data Fusion Symposium, ADFS '96*, pages 184–189, Newport, RI, November 1996.

[15] M. Krieg and D. Gray. Multi-sensor, probabilistic multi-hypothesis tracking. In *Data Fusion Symposium, ADFS 96*, pages 153–158, Salisbury, Australia, November 1996.

[16] Streit R. and Luginbuhl T. Probabilistic multi-hypothesis tracking. Technical Report 10428, NUWC-NPT, Newport, RI, 1995.

[17] C. Rago, P. Willett, and R. Streit. Direct data fusion using the PMHT. In *Proceedings of American Control Conference*, volume 3, pages 1698–1702, Storrs, CT, June 1995.

[18] X. Song, J. Cui, H. Zha, and H. Zhao. Probabilistic detection-based particle filter for multi-target tracking. In *Proc. of British Machine Vision Conference*, pages 223–232, 2008.

[19] P. Willett, Y. Ruan, and R. Streit. PMHT: Problems and some solutions. *IEEE Trans. on Aerospace and Electronic Systems*, 38(3): 738–754, 2002.

Sora Choi received her Ph.D. degree, in Mathematics, from Seoul National University, Seoul, Korea in 2003. She was a researcher at the Electronics and Telecommunications Research Institute (ETRI), Daejeon, Korea from 2003 to 2004, and was an instructor at Seoul National University between 2000 and 2002, Kyunghee and Konkuk Universities, in Korea, in 2007. She received a Graduate Predoctoral Fellowship in 2011 and Ph.D. in Electrical Engineering at the University of Connecticut, Storrs in 2013. She is currently working in the Department of Electrical Engineering and Computer Science in Syracuse University, Syracuse, NY as a Post Doctorate Research Associate. Her research interests are in sensor fusion, detection theory, target tracking, signal processing, and fault diagnosis.

Peter Willett (F'03) received his B.A.Sc. (Engineering Science) from the University of Toronto in 1982, and his Ph.D. degree from Princeton University in 1986.

He has been a faculty member at the University of Connecticut ever since, and since 1998 has been a Professor. His primary areas of research have been statistical signal processing, detection, machine learning, data fusion and tracking. He has interests in and has published in the areas of change/abnormality detection, optical pattern recognition, communications and industrial/security condition monitoring.

He is editor-in-chief for IEEE Signal Processing Letters and is VP Publications for the IEEE AES Society. He was until recently EIC of the *IEEE Transactions on AES*, and associate editor for *IEEE Transactions on Systems, Man, and Cybernetics*, parts A and B, *IEEE AES Magazine*, and ISIF's *Journal of Advances in Information Fusion*. He was General Co-Chair for the 2006 ISIF/IEEE Fusion Conference in Florence, for 2008 in Cologne and for 2011 in Chicago. He was Program Co-Chair for the 2003 IEEE Conference on Systems, Man, and Cybernetics in Washington DC, and for the 1999 Fusion Conference in Sunnyvale.

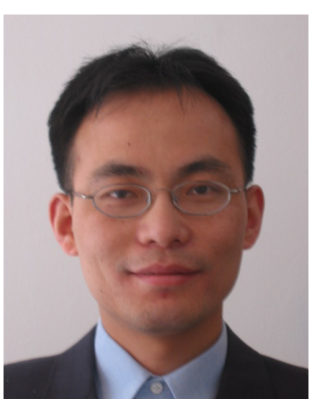

Shengli Zhou (IEEE Fellow 2014) received the B.S. degree in 1995 and the M.Sc. degree in 1998, from the University of Science and Technology of China (USTC), Hefei, China, both in electrical engineering and information science. He received his Ph.D. degree in electrical engineering from the University of Minnesota (UMN), Minneapolis, USA, in 2002.

He is now a full professor with the Department of Electrical and Computer Engineering at the University of Connecticut (UCONN), Storrs, USA. He has held a United Technologies Corporation (UTC) Professorship in Engineering Innovation, 2008–2011, and the Charles H. Knapp Associate Professor in Electrical Engineering, 2012–2013. His general research interests lie in the areas of wireless communications and signal processing. His recent focus is on underwater acoustic communications and networking.

Dr. Zhou has served as an Associate Editor for IEEE Transactions on Wireless Communications, 2005–2007, for IEEE Transactions on Signal Processing, 2008–2010, and now is an associate editor for IEEE Journal of Oceanic Engineering. He received the 2007 ONR Young Investigator award and the 2007 Presidential Early Career Award for Scientists and Engineers (PECASE). He is a member of the Connecticut Academy of Science and Engineering (CASE), and has been recently elected to IEEE Fellow.